Chapter 10
Formation of a Narrow Group of Intense Lines in the Emission and Photoexcitation Spectra

R. Karazija, S. Kučas, V. Jonauskas, and A. Momkauskaitė

Abstract Formation of a narrow group of intense lines in the emission and photoexcitation spectra, corresponding to the transitions between the electron shells with the same principal quantum number is considered. There are two reasons of such an effect, namely, the strong Coulomb exchange interaction and the configuration interaction with a symmetric exchange of symmetry. The conditions and regularities of their manifestation in the isoelectronic and isonuclear sequences are analyzed.

10.1 Introduction

The excited configurations of atoms, containing two open shells with the same principal quantum number, are distinguished by some particular features. The radial orbitals of such neighboring shells overlap considerably, thus, the Coulomb interaction between these shells remains more important than the spin-orbit interaction even in the highly charged ions of heavy elements (namely, such a case will be considered in our paper). The exchange part of the Coulomb interaction depends more on the overlap of orbitals than the direct interaction, thus, the strong exchange interaction mainly forms the structure of energy level spectrum and determines its rather large width.

Configuration of such a type is obtained by the dipole excitation from the closed shell nl^{4l+2} to the outer open shell $n(l+1)^N$. The two different cases can be distinguished:

R. Karazija (✉) · S. Kučas · V. Jonauskas · A. Momkauskaitė
Institute of Theoretical Physics and Astronomy, Vilnius University, A. Goštauto 12, 01108 Vilnius, Lithuania
e-mail: romualdas.karazija@tfai.vu.lt

S. Kučas
e-mail: sigitas.kucas@tfai.vu.lt

V. Jonauskas
e-mail: valdas.jonauskas@tfai.vu.lt

A. Momkauskaitė
e-mail: alina.momkauskaite@tfai.vu.lt

M. Mohan (ed.), *New Trends in Atomic and Molecular Physics*,
Springer Series on Atomic, Optical, and Plasma Physics 76,
DOI 10.1007/978-3-642-38167-6_10,

(i) If $l = n - 2$, the other excited configuration $nl^{4l+2}n(l+1)^{N-1}n(l+2)$, belonging to the same complex, does not exist. Then usually the main features of transition array

$$nl^{4l+2}n(l+1)^N - nl^{4l+1}n(l+1)^{N+1} \tag{10.1}$$

can be described by the single-configuration approximation.

(ii) If $l \leq n - 3$, the $nl^{4l+2}n(l+1)^{N-1}n(l+2)$ configuration is possible and it strongly interacts with the $nl^{4l+1}n(l+1)^{N+1}$ configuration. In the second configuration one electron is filling the vacancy in a deeper shell with a smaller orbital quantum number and the other electron is excited to an empty shell with a larger orbital quantum number, thus, this configuration interaction (CI) is named as the interaction with a symmetric exchange of symmetry (SEOS) [1]. Both these excited configurations are related by the electric dipole transitions to the ground configuration; thus, their interaction strongly influences the transition array:

$$nl^{4l+2}n(l+1)^N - \left(nl^{4l+1}n(l+1)^{N+1} + nl^{4l+2}n(l+1)^{N-1}n(l+2)\right). \tag{10.2}$$

The short notation n–n for such transitions is used.

The first striking manifestation of the Coulomb exchange interaction influence on the photoabsorption spectra was obtained in the late sixties. The registered 4d photoabsorption spectra of lanthanide metals are dominated by one broad peak instead of usual for the photoionization from an inner shell saw-tooth shape [2]. These spectra were interpreted in a free-ion model as the giant resonances corresponding to the excitation from the $4d^{10}$ shell to the open $4f^N$ shell [3–5]. The resonance is formed by a few intense overlapping lines, concentrated on a short-wavelength side of the spectrum. The 4d spectra of free atoms also contain the similar giant resonances [6], though their interpretation at the beginning of the group is complicated by the problem of the collapse of $4f$ orbital [7, 8]. It was suggested in [3, 9] that the strongest photoexcitation lines correspond to the transitions into the upper group of levels, formed by the Coulomb exchange interaction. Cancellation of many lines on the low-energy side of the spectrum, corresponding to transitions (10.1), was related to the existence of additional selection rule for a number of vacancy-electron pairs in the special wavefunction basis [10]. The giant resonances are also typical of the photoabsorption from the $3d^{10}$ shell in the vapors of elements from the second part of the iron group [11, 12]. However, the single-configuration model becomes inaccurate for the $3p$ photoabsorption spectra of the elements from the first part of this group: due to the near-degeneracy of $3d$ and $4s$ orbitals and strong $(s+d)^N$ mixing, they contain a large number of sharp resonances also on the high-energy side.

The main feature of the photoexcitation and emission spectra, corresponding to transitions (10.2), is also the formation of a narrow group of intense lines (NGIL) and quenching of many other lines due to CI SEOS. This effect at first was noticed in [13–15] for the spectra corresponding to 3–3 transitions. The strong resonance-like emission of laser-produced plasma involving elements from Cs to Yb was reported in [16, 17] and attributed to 4–4 transitions at ionization degrees $q = 7$–15.

Under the assumption that the intensities of emission lines can be approximated by their strengths the closed formula was derived for the shift of average energy of transition array due to CI [18]. This formula demonstrates that such a shift due to CI SEOS is mainly determined by the dipole term of the interconfigurational Coulomb interaction and is always positive. The concepts of the emissive and receptive zones were introduced as the line-strength-weighted energy level distribution of the upper and lower configurations [19].

NGIL in the spectra of plasma obtains the form of unresolved transition array or quasi-continuum band. Such bands attracted much attention due to their applications. The emission spectra of highly charged ions are considered as a prospective source of EUV and XUV radiation for lithography [20, 21]. For this reason the extensive investigations of band formation in the spectra of Sn^{q+} ions at 13.5 nm [20, 22–25] as well as in the Gd^{q+} and Tb^{q+} ions at 6.5 nm [21, 26, 27] have been performed. On the other hand, such a radiation in the highly charged tungsten ions plays a negative role [28, 29], as it causes large radiation losses in the tokamak plasma. The separate intense lines of less complex spectra of ions, corresponding to 3–3 transitions, are widely used for diagnostics of laboratory and astrophysics plasma [30].

In the low density plasma, obtained in tokamak or EBIT, the ground level of ions is mainly populated. Under these conditions the influence of CI SEOS on the emission and excitation spectra does not necessarily obey the same regularities as in the case of the total transition arrays. The formation of narrow groups of intense lines for such emission and photoexcitation spectra corresponding to 4–4 and 3–3 transitions in the isoelectronic an isonuclear sequences was investigated in [31, 32].

Two possible mechanisms of the formation of NGIL are considered in Sects. 10.2 and 10.3 of this work.

The results of calculations presented in this work were obtained in the single-, two- or many-configuration approximations with quasi-relativistic Hartree-Fock (HFR) [33], relativistic Dirac-Fock-Slater (RDFS) [34] and relativistic Dirac-Fock (RDF) [35] wave functions. All relativistic configurations corresponding to the same nonrelativistic configuration were taken into account.

10.2 Formation of a Narrow Group of Intense Lines by the Coulomb Interaction in the Single-Configuration Approximation

Even in rather heavy atoms and highly charged ions the structure and width of the energy level spectrum of $nl_1^{N_1} nl_2^{N_2}$ configuration mainly depend on the exchange part of the Coulomb interaction. In the second quantization representation the operator of this interaction between two open shells can be presented in the form [9]:

$$H_{\mathrm{ex}}^{C}=\left(\sum_{k}\bigl(C^{(k)}(nl_1,nl_2)C^{(k)}(nl_2,nl_1)\bigr)-\frac{\hat{N}(nl_2)}{2l_2+1}\right)\times\langle l_1\|C^{(k)}\|l_2\rangle^2 G^k(nl_1,nl_2). \tag{10.3}$$

Here, $C^{(k)}(nl_1,nl_2)$ is the spherical tensor of rank k producing the exchange of electron between shells:

$$C_q^{(k)}(nl_1,nl_2)=\sum_{\nu\xi}a_\nu^{+}\langle nl_1\nu|C_q^{(k)}|nl_2\xi\rangle b_\xi, \tag{10.4}$$

a_ν^{+} is the operator of electron creation in the state $nl_1\nu$ and b_ξ is the operator of electron annihilation in the state $nl_2\xi$, where ν and ξ denote the sets of orbital and spin momenta projections. In Eq. (10.3), $\hat{N}(nl_2)$ is the operator of electron number in the shell $nl_2^{N_2}$ and its eigenvalue is equal to N_2. $G^k(nl_1,nl_2)$ is the exchange radial integral, and the multiplier before it is the reduced matrix element of spherical tensor of rank k.

The main contribution to the matrix element of the H_{ex}^{C} operator is given by the smallest order term in its expansion. When $l_2=l_1+1$, such a term is the dipole one with $k=1$. The $C^{(1)}(nl_1,nl_2)$ operator represents the electric dipole transition operator, but acting only in the spin angular space. Consequently, the matrix element of the H_{ex}^{C} operator can be expressed in terms of dipole transition amplitudes (without the radial integral). In the case of two considered excited configurations the g_1 coefficient at the Slater integral $G^1(nl_1,nl_2)$ obtains the following expressions [9]:

$$\begin{aligned}
&g_1\bigl(l^{4l+1}(l+1)^{N+1}\gamma_2L_2S_2,\gamma_2'L_2'S_2'LS\bigr)\\
&\quad=(2J+1)^{-1}\sum_{\gamma_2''L_2''S_2''L'S'J'}\bigl\langle l^{4l+1}(l+1)^{N+1}(\gamma_2L_2S_2)LSJ\\
&\qquad\times\bigl\|C^{(1)}\bigr\|l^{4l+2}(l+1)^{N}\bigl(\gamma_2''L_2''S_2''\bigr)L'S'J'\bigr\rangle\\
&\qquad\times\bigl\langle l^{4l+1}(l+1)^{N+1}\bigl(\gamma_2'L_2'S_2'\bigr)LSJ\bigl\|C^{(1)}\bigr\|l^{4l+2}(l+1)^{N}\bigl(\gamma_2''L_2''S_2''\bigr)L'S'J'\bigr\rangle\\
&\qquad-\delta\bigl(\gamma_2L_2S_2,\gamma_2'L_2'S_2'\bigr)\frac{N+1}{2l+3}\langle l\|C^{(1)}\|l+1\rangle^2;
\end{aligned}\tag{10.5}$$

$$\begin{aligned}
&g_1\bigl((l+1)^{N-1}\gamma_1L_1S_1,\gamma_1'L_1'S_1'(l+2)LS\bigr)\\
&\quad=(2J+1)^{-1}\sum_{\gamma_1''L_1''S_1''L'S'J'}\bigl\langle(l+1)^{N-1}\gamma_1L_1S_1(l+2)LSJ\\
&\qquad\times\bigl\|C^{(1)}\bigr\|(l+1)^{N}\bigl(\gamma_1''L_1''S_1''\bigr)L'S'J'\bigr\rangle\\
&\qquad\times\bigl\langle(l+1)^{N-1}\gamma_1'L_1'S_1'(l+2)LSJ\bigl\|C^{(1)}\bigr\|(l+1)^{N}\bigl(\gamma_1''L_1''S_1''\bigr)L'S'J'\bigr\rangle\\
&\qquad-\delta\bigl(\gamma_2L_2S_2,\gamma_2'L_2'S_2'\bigr)\frac{1}{2l+5}\langle l+1\|C^{(1)}\|l+2\rangle^2.
\end{aligned}\tag{10.6}$$

The dependence of the right-hand side of Eqs. (10.5) and (10.6) on the total quantum number J disappears when the summation over J' is performed.

Table 10.1 Number of terms in the upper and lower groups of some configurations with two open shells

Configuration	p^5d	p^4d	p^3d	p^2d	pd	d^9f	d^8f	d^7f	d^6f	d^9f^2	d^9f^3
All terms	6	12	18	12	6	10	33	88	118	42	158
Upper terms after diagonalization	1	3	8	7	5	1	3	13	24	3	20
Lower terms before diagonalization	5	6	6	3	1	9	21	33	21	27	49
after diagonalization	5	9	10	5	1	9	30	75	94	39	138

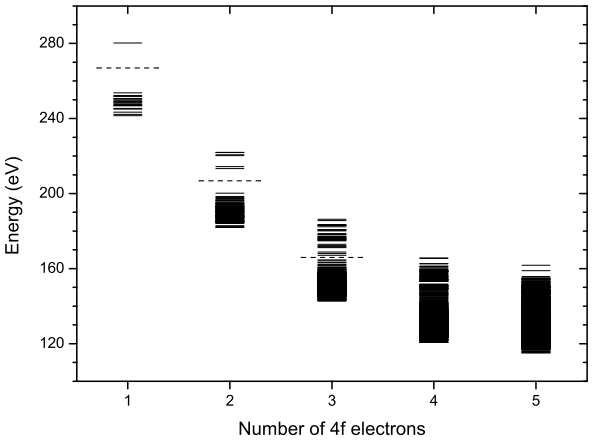

Fig. 10.1 Two groups of levels in the energy level spectra for the isonuclear sequence of praseodymium $4d^94f^N$ ($N = 1$–5). Both groups are energetically separated only for $N = 1$–3, this is indicated by a *broken line*. Results of calculations in the single-configuration HFR approximation

Thus, the g_1 coefficient consists of the term-dependent and term-independent parts. For the diagonal matrix element the term-dependent part has a positive value. It gives a contribution to the energy only for those terms of $nl^{4l+1}n(l+1)^{N+1}$ or $n(l+1)^{N-1}n(l+2)$ configuration, which are related by the electric dipole transitions to the terms of $nl^{4l+2}n(l+1)^N$ configuration. Consequently, the terms of excited configuration have a tendency to separate into two groups: the lower group with a negative and constant g_1 value and the upper group, corresponding to a positive term-dependent g_1 coefficient.

The nondiagonal g_1 coefficients can also obtain rather large values of the same order as the diagonal ones. However, only terms of the upper group are mixed among themselves due to the exchange interaction. This interaction shifts some terms of this group to the lower one. The numbers of terms belonging to the upper and lower groups before and after the diagonalization of $\|g_1\|$ matrix are indicated in Table 10.1.

The separation of energy levels by the Coulomb exchange interaction into two groups is illustrated in Fig. 10.1 for the energy level spectra of $4d^94f^N$ config-

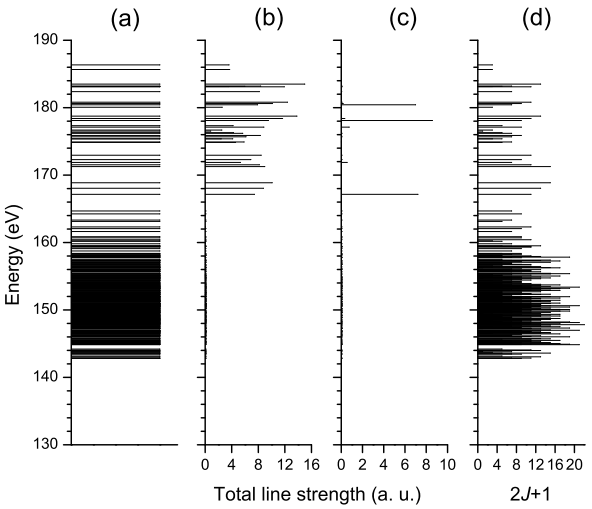

Fig. 10.2 Energy level spectrum of the Pr^{3+} $4d^9 4f^3$ (**a**) and the total line strength of transitions from each of these levels: to all levels of the $4d^{10}4f^2$ configuration (**b**); to the ground level of this configuration (**c**); proportional to $2J + 1$ (equal from all states) (**d**). Results of calculations in the single-configuration HFR approximation

urations ($N = 1$–5). The levels of both groups are separated energetically for the configurations with a small number of electrons in the second shell. On increasing N these groups approach and overlap each other. At $N = 1$, there is only one level $^1P_1$ of the upper group, situated distantly from the other 19 levels. At $N = 2$, the upper group is formed by the six levels of three terms $(^3_2H)^2F$, $(^3_2F)^2D$ and $(^3_2H)^2G$, the total number of levels is 109. At $N = 3$, the upper group (35 levels) remains separated yet by a small energy gap from the numerous lower group (351 levels). For the larger number of $4f$ electrons the levels of both groups are distinguished only by their deexcitation rates.

Taking into account entirely the dipole part of matrix element, only levels of the upper group are involved in the electric dipole transitions. Additionally, a higher position of term correlates with a larger transition rate to/from the levels of the ground configuration. The concentration of transition rate from the levels of $4d^9 4f^3$ configuration to all levels and only to the ground level of $4d^{10}4f^2$ configuration in the intermediate coupling is shown in Fig. 10.2. For comparison the equally probable deexcitation of all states (the deexcitation rate of level proportional to its statistical weight $2J + 1$) is shown too. Thus, the formation of NGIL is typical of the whole array of transitions between both configurations as well as of the excitations from the ground level. The first case corresponds to the emission spectrum at the statistical populations of excited levels. The second case corresponds to the photoexcitation spectrum, which is usually excited only from the ground level.

Consequently, the transitions between the excited and ground configurations tend to concentrate on a shorter wavelength side of the spectrum. Of course, the calculation in the intermediate coupling gives some probabilities of lines to/from the levels of the lower group as well, but usually their values are essentially smaller (Fig. 10.3).

The calculated distribution can be closely approximated using the new wavefunction basis, obtained by the diagonalization of $\|g_1\|$ matrix [3, 9]. In an algebraic way such a basis can be constructed using the special operator, which creates a vacancy

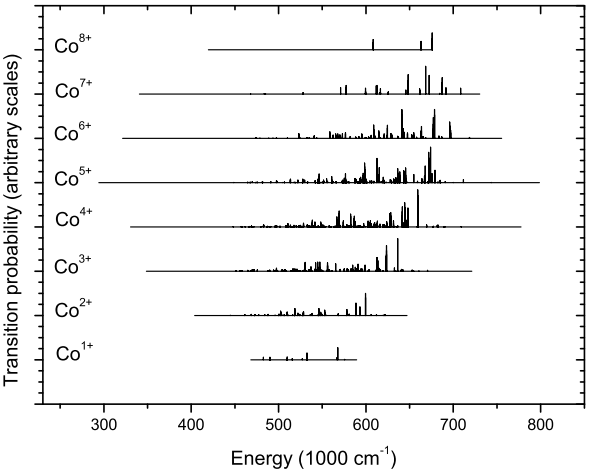

Fig. 10.3 Probabilities of radiative transitions $3p^5 3d^{N+1}$–$3p^6 3d^N$ in the Co^{q+} isonuclear sequence [10]. The *horizontal sections of graphs* indicate the intervals of possible transition energies

in one shell and an electron in the other shell, thus, the wavefunction of the excited configuration is obtained [10, 36]. Such a vacancy-electron pair is coupled to the ^{1}P term. The lowest configuration with the same number of electrons has no vacancies in the first shell. When acting with this operator repeatedly, the various states of the sequence of configurations with a different number of vacancy-electron pairs p can be obtained. Thus, a new quantum number p is introduced for the classification of states by the parentage in such a configuration sequence. It was shown in [10] that the additional selection rule appears in this hole-particle basis: the electric dipole transitions are possible only between the states, differing in this quantum number by unity $\Delta p = 1$.

In order to characterize the different role of energy levels of considered configuration in the transitions to the other configuration the concept of emissive zone was introduced [19]. It is defined using the statistical moments of the energy level spectrum, calculated taking into account the participation of energy levels in these transitions. In order to obtain their algebraic expressions two assumptions are made: (i) the excited levels are populated statistically and (ii) the line intensities are proportional to the line strengths. The average energy of the emissive zone for configuration K corresponding to the transitions into configuration K' was defined in [19]:

$$\bar{E}_{K'}(K) = \frac{\sum_{\gamma\gamma'} \langle K\gamma|H|K\gamma\rangle S(K\gamma, K'\gamma')}{S(K, K')}, \tag{10.7}$$

where $S(K\gamma, K'\gamma')$ is the line strength of transition between the levels γ and γ'. The quantity in the denominator is the total line strength. It is useful to determine the position of zone with respect to the average energy of configuration $\bar{E}(K)$. For the pair of the excited and ground configurations this shift of average energy has the following explicit expression [19]:

$$\delta\bar{E}_{K_0 nl_1^{N_1+1} nl_2^{N_2-1}}\left(K_0 nl_1^{N_1} nl_2^{N_2}\right)$$
$$= -\frac{N_1(4l_2+2-N_2)}{(4l_1+1)(4l_2+1)}\left\{\left[\frac{2}{3}\delta(k,1) - \frac{1}{2(2l_1+1)(2l_2+1)}\right]\right.$$
$$\times (-1)^k \langle l_1 \| C^{(k)} \| l_2\rangle^2 G^k(nl_1, nl_2)$$
$$\left. + \sum_{k>0} \begin{Bmatrix} l_1 & l_1 & k \\ l_2 & l_2 & 1 \end{Bmatrix} \langle l_1 \| C^{(k)} \| l_1\rangle \langle l_2 \| C^{(k)} \| l_2\rangle F^k(nl_1, nl_2)\right\}, \quad (10.8)$$

where K_0 means the passive closed shells.

Analysis of Eq. (10.8) confirms that the dipole exchange term mainly determines the concentration of line strength in the transitions from the upper levels. The shift of emissive zone is always positive because the first term in the brackets exceeds the second negative term. This shift obtains the largest value at $N_2 = 1$ and decreases by increasing N_2.

Also the second moment of emissive zone—the variance can be introduced:

$$\sigma^2_{K'}(K) = \frac{\sum_{\gamma\gamma'}[\langle K\gamma|H|K\gamma\rangle - \bar{E}_{K'}(K)]^2 S(K\gamma, K'\gamma')}{S(K, K')}. \quad (10.9)$$

It has more complex expression which is given in [37]. The knowing of variance enables one to determine the width of zone as the full width at the half maximum of the normal distribution:

$$\Delta E_{K'}(K) = 2\sqrt{2\ln 2\sigma^2_{K'}(K)}. \quad (10.10)$$

The examples of emissive zones, calculated using such a model, were given in [19, 37]. Certainly, the zones for the same configuration, but corresponding to the transitions to the different final configurations, do not coincide and can essentially differ. The interval of zone, determined by Eqs. (10.7), (10.9) and (10.10), corresponds rather approximately to the position of the upper group of levels; the emissive zone can be obtained even beyond the interval of energy level spectrum of configuration [19].

Similarly, the receptive zone, corresponding to the final configuration of transition can be introduced.

It is necessary to note that the same term *emissive zone* is also used in other sense: the interval of emission lines with the transition probabilities greater then a certain given value [21].

10.3 Formation of a Narrow Group of Intense Lines by the Configuration Interaction

In this section we will consider the conditions and regularities of NGIL formation for transitions (10.2) in the isoelectronic and isonuclear sequences. Spectra of ions can be recorded at various conditions: in laser-produced plasma, EBIT, vacuum spark, Large Helical Device and other devices. It is necessary to distinguish the manifestation of this effect in two types of spectra:

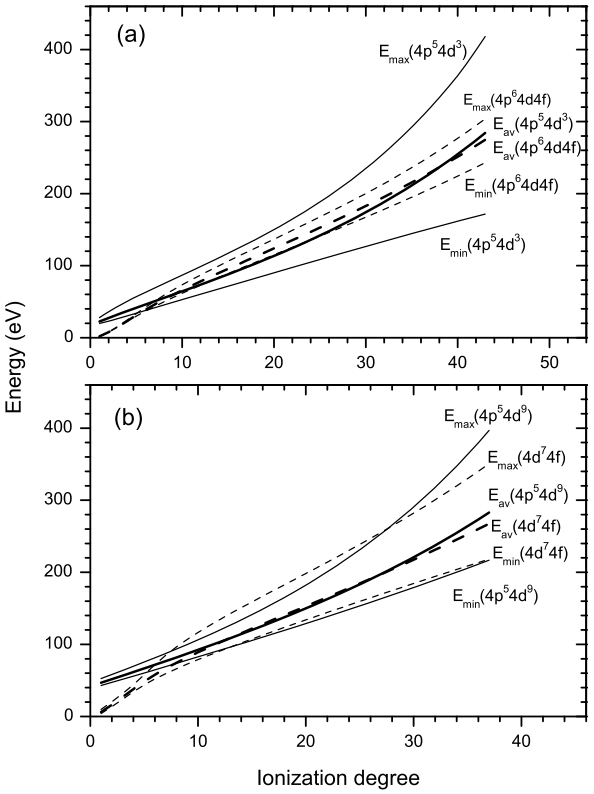

Fig. 10.4 Overlap of the energy level spectra of the $4p^5 4d^3$ and $4p^6 4d4f$ configurations in the Sr isoelectronic sequence (**a**) and of the $4p^5 4d^9$ and $4p^6 4d^7 4f$ configurations in the Ru isoelectronic sequence (**b**) [31]. Average energy (E_{av}), upper (E_{max}) and lower (E_{min}) limits of the spectrum are given with respect to the ground level of the corresponding ion. Results of calculations in the single-configuration HFR approximation

(i) In a plasma of high density at local thermodynamic equilibrium the intensities of emission lines are proportional to the transition rates. The wavelengths of considered transitions for the ions correspond to VUV or X-ray regions, thus, the transition energy exceeds the interval of energy level spectrum and the transition rate can be approximated by the line strength.

(ii) In a plasma of low density, typical of EBIT or tokamak, only the ground level of ions is mainly populated. Thus, the important processes are the dipole excitation from the ground level of $nl^{4l+2}n(l+1)^N$ configuration as well as the subsequent emission after such an excitation.

The main interest presents the formation of NGIL in the emission and photoexcitation spectra of ions, corresponding to the transitions:

$$\left(3s3p^{N+1} + 3s^2 3p^{N-1}3d\right) - 3s^2 3p^N, \tag{10.11}$$

$$\left(4p^5 4d^{N+1} + 4p^6 4d^{N-1}4f\right) - 4p^6 4d^N. \tag{10.12}$$

These cases are considered in our review.

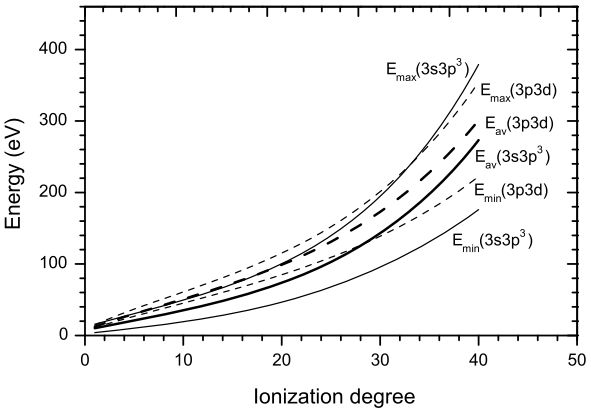

Fig. 10.5 Overlap of the energy level spectra of the $3s3p^3$ and $3s^23p3d$ configurations in the Si isoelectronic sequence [32]. Average energy (E_{av}), upper ($E_{\max}$) and lower ($E_{\min}$) limits of the spectrum are given with respect to the ground level of $3s^23p^2$ configuration. Results of calculations in the HFR single-configuration approximation

10.3.1 Overlap of the Energy Level Spectra of the $nl^{4l+1}n(l+1)^{N+1}$ and $nl^{4l+2}n(l+1)^{N-1}n(l+2)$ Configurations. Validity of the Two-Configuration Model

Both excited configurations overlap considerably at various numbers of electrons N and ionization degrees q (Figs. 10.4 and 10.5). At small numbers of N, the larger width has the energy level spectrum of $nl^{4l+1}n(l+1)^{N+1}$ configuration with more filled outer shell. At large numbers of N, the spectrum of $nl^{4l+2}n(l+1)^{N-1}n(l+2)$ configuration tends to expand more than the spectrum of $nl^{4l+1}n(l+1)^{N+1}$ configuration.

In neutral atoms, the average energy of $nl^{4l+1}n(l+1)^{N+1}$ configuration exceeds that of $nl^{4l+2}n(l+1)^{N-1}n(l+2)$ configuration. However, in the isoelectronic sequence on increasing ionization degree the collapse of $\mathrm{P}_{n(l+2)}(r)$ radial orbital and its further contraction take place (Fig. 10.6). The interaction of this electron with the $n(l+1)^{N-1}$ shell becomes stronger, which upraises the energy level spectrum of $nl^{4l+2}n(l+1)^{N-1}n(l+2)$ configuration; thus, the average energies of both configurations interchange. At large numbers of q, the average energies of two configurations become closer again ($n=3$) and even intersect the second time ($n=4$); the reason is a different number of 4d electrons, interacting with a vacancy and an excited electron [31].

The fast contraction of the $\mathrm{P}_{n(l+2)}(r)$ radial orbital also strongly influences the variation of the line strength of $n(l+1)-n(l+2)$ transitions in the isoelectronic sequence (Fig. 10.7). The total line strength of these transitions resonantly increases at the beginning of the sequence, obtains its maximal value and fast decreases further on. The sharper resonance is obtained for the smaller orbital quantum number of $n(l+2)$ electron and for the more filled $n(l+1)^{N-1}$ shell. It is necessary to note that the configuration mixing does not change the total line strength of both transition arrays, calculated in the single-configuration approximation.

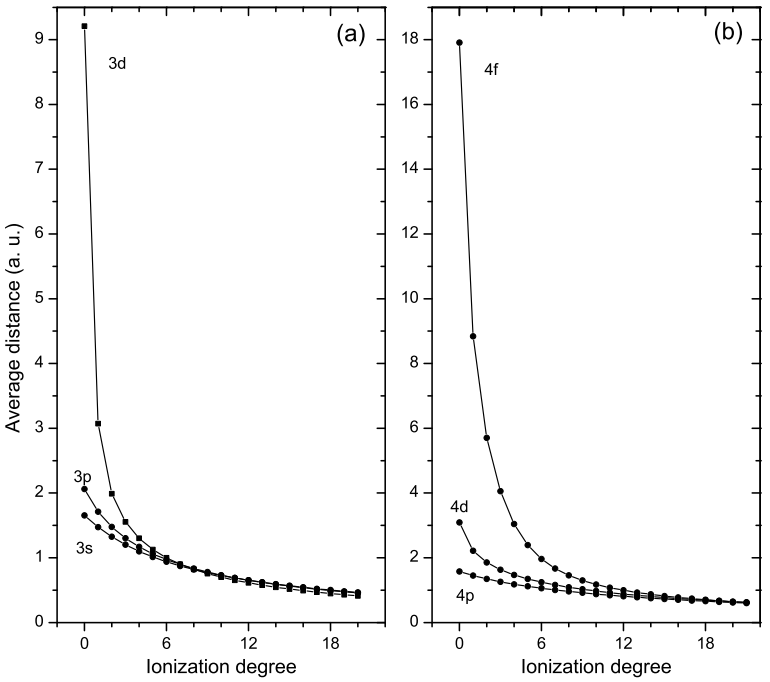

Fig. 10.6 Dependence of the average distance of electrons from the nucleus on the ionization degree: (**a**) in the S $3s^2 3p^3 3d$ isoelectronic sequence [32]; (**b**) in the Tc $4p^6 4d^6 4f$ isoelectronic sequence [31]. Results of calculations in the single-configuration HFR approximation

In neutral atoms and first ions the considered excited configurations are also mixed with other configurations, but from the ionization degree $q \approx 5$ the formation of NGIL is properly determined by SEOS in the two-configuration approximation. It was demonstrated in [24, 31, 32] by the comparison of various spectra, calculated in the single-configuration and two-configuration approximations, with the results of more exact calculations using a wider basis of wavefunctions or semi-empirical values of the radial integrals. Some examples are presented in Figs. 10.8 and 10.9. The spectrum of two transition arrays, calculated in the single-configuration approximation, does not resemble a real spectrum at all.

Though the energy level spectra of both excited configurations strongly overlap, their main lines usually are situated distantly. Taking into account the strong CI SEOS the most lines with the longer wavelengths are canceled and the line strength is concentrated in a few intense lines on the shorter wavelength side of the spectrum. Thus, a fairly good agreement with the results of more exact calculation of the spectrum is obtained.

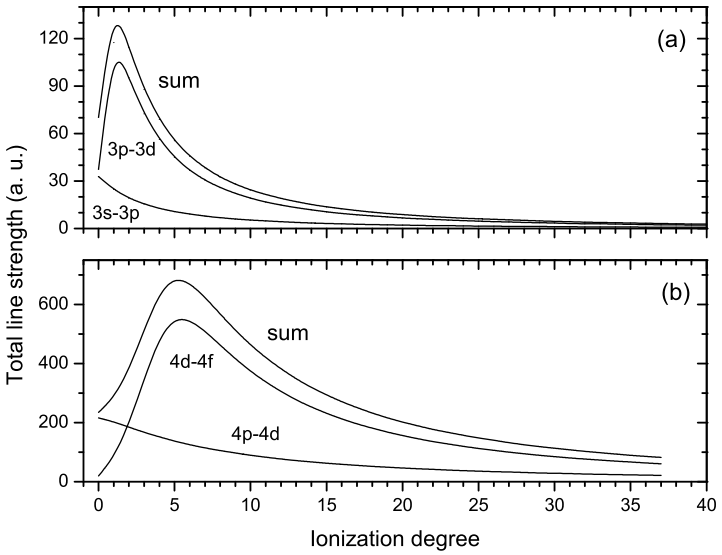

Fig. 10.7 Dependence of the total line strength of transitions (10.2) on the ionization degree: (**a**) $3s3p^5$–$3s^23p^4$, $3s^23p^33d$–$3s^23p^4$ and $(3s3p^5 + 3s^23p^33d)$–$3s^23p^4$ transitions in the S isoelectronic sequence [32]; (**b**), and $4p^54d^8$–$4p^64d^7$, $4p^64d^64f$–$4p^64d^7$ and $(4p^54d^8 + 4p^64d^64f)$–$4p^64d^7$ transitions in the Tc isoelectronic sequence [31]. Results of calculations in the single-configuration and two-configuration HFR approximations

10.3.2 Formation of NGIL in the Spectra with the Intensities of Lines Proportional to the Line Strength

The approximate explicit expression for intensity of line enables one to obtain the closed formula of the average energy and other mean characteristics of transition array. Their analysis reveals some general regularities of NGIL formation in corresponding spectra.

The average energy of such a transition array equals the difference of average energies of emissive and receptive zones for the initial and final configurations:

$$\bar{E}\big(K - K'\big) = \bar{E}_{K'}(K) - \bar{E}_K\big(K'\big). \tag{10.13}$$

The influence of CI SEOS on the line strength distribution can be estimated by the difference of its average energy in the two-configuration and single-configuration approximations. For transitions (10.2) it obtains the following expressions [18]:

$$\begin{aligned}
&\Delta E_{\mathrm{CI}}\big(\big(K_0 nsnp^{N+1} + K_0 ns^2 np^{N-1} nd\big) - K_0 ns^2 np^N\big) \\
&\quad = \frac{4}{15}\,\frac{N(6-N)\langle ns|r|np\rangle\langle np|r|nd\rangle}{2N\langle np|r|nd\rangle^2 + (6-N)\langle ns|r|np\rangle^2} R^1(nsnd, npnp); \\
&\Delta E_{\mathrm{CI}}\big(\big(K_0 np^5 nd^{N+1} + K_0 np^6 nd^{N-1} nf\big) - K_0 np^6 nd^N\big)
\end{aligned} \tag{10.14}$$

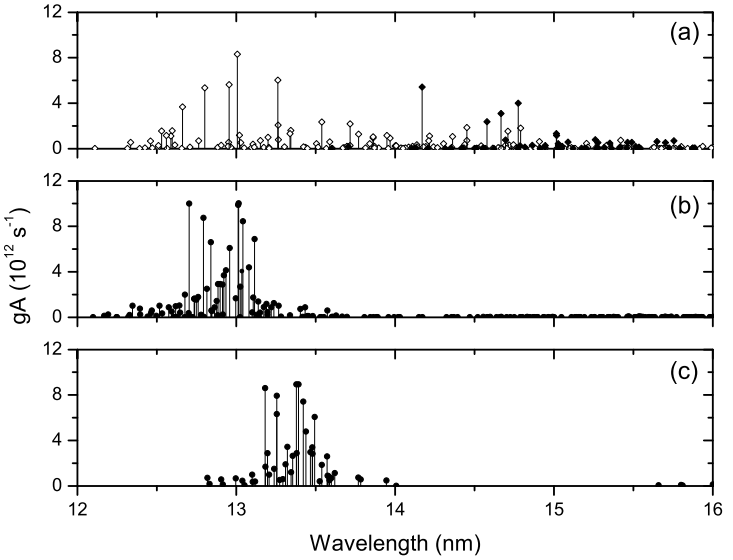

Fig. 10.8 Distribution of the probabilities of transitions $(4p^5 4d^3 + 4p^6 4d 4f)$–$4p^6 4d^2$ for Sn^{12+}, calculated in the single-configuration RDFS approximation (**a**), two-configuration RDFS approximation (**b**) [39] and semi-empirically (**c**) [38]. In (**a**) the lines of transitions from the $4p^5 4d^3$ configuration levels are indicated by *solid diamonds* and from $4p^6 4d 4f$ configuration by *open diamonds*

$$= \frac{4}{15} \frac{N(10-N)\langle np|r|nd\rangle \langle nd|r|nf\rangle}{3N\langle nd|r|nf\rangle^2 + 2(10-N)\langle np|r|nd\rangle^2} \times \left(\frac{7}{3}R^1(npnf, ndnd) - \frac{2}{7}R^3(npnf, ndnd)\right). \quad (10.15)$$

Here, $\langle nl|r|nl'\rangle$ is the radial integral of dipole transition and R^k is the interconfigurational radial integral of the Coulomb interaction. The shift ΔE_{CI} as well as the shift (10.8) is also mainly determined by the dipole term with $k = 1$. The radial orbitals $P_{nl}(r)$ and $P_{n(l+1)}(r)$ have a different sign in the region of their main maxima, thus, the radial transition integral $\langle nl|r|n(l+1)\rangle$ obtains a negative value and the interconfigurational radial integral R^k—a positive value. Consequently, the shift of average energy due to CI SEOS is always positive. As was demonstrated in Figs. 10.4 and 10.5, the energy spectra of both excited configurations strongly overlap at various ionization degrees, but the intense lines of both arrays do not necessarily overlap too. If they are situated separately, SEOS configuration mixing enhances the shorter wavelength transitions from the higher configuration and quenches the longer wavelength transitions from the lower configuration; such an example is given in Fig. 10.8. Depending on the atomic number and ionization degree the intense lines of the first or the second transition arrays have longer wavelengths, thus, NGIL can be formed in a region of one or the other array. Such a role of two arrays in CI SEOS can be changed not only in the isoelectronic, but also

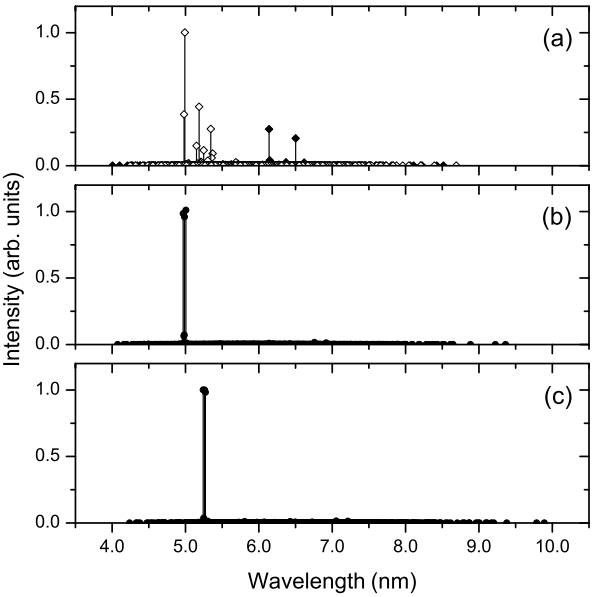

Fig. 10.9 Emission spectrum of W^{31+} around 5 nm after the photoexcitation from the ground level of $4p^64d^7$ configuration [31]. (**a**) Transitions $4p^54d^8$–$4p^64d^7$ (*solid diamonds*), $4p^64d^64f$–$4p^64d^7$ (*open diamonds*) in the single-configuration approximation. (**b**) The mixed array of $(4p^54d^8 + 4p^64d^64f)$–$4p^64d^7$ transitions in the two-configuration approximation. (**c**) Spectrum obtained taking into account eight additional configurations, namely, $4p^54d^64f^2$, $4p^54d^64f5p$, $4p^64d^44f^3$, $4p^64d^54f(5d + 5g)$, $4p^44d^84f$, $4p^44d^64f^3$ for the initial excited state, and $4p^64d^54f^2$ for the ground state. Results of the RDFS calculations

in the isonuclear sequence, for example, in the Pr^{q+} [18] or Gd^{q+} and Tb^{q+} [26] sequences on decreasing a number of electrons in the $4d^N$ shell.

Another regularity of CI SEOS influence on transition array, manifesting itself in the various isonuclear sequences, is a very slow variation of the mean wavelength on increasing the ionization degree, while the mean wavelength of one and the other array changes reasonably [18, 40, 41].

It is necessary to note that the formation of NGIL does not manifest itself at all if some levels of the lower configuration with the large deexcitation rates are not related by the interconfiguration matrix elements to the levels of the upper configuration and thus some intense lines on a long-wavelength side of the spectrum remain unaffected by CI SEOS. For example, it takes place at the beginning of isoelectronic sequences when the intense lines, originating from the $nl^{4l+1}n(l+1)^{4l+5}$ configuration with a few terms, have the shorter wavelengths than the intense lines, originating from the more complex $nl^{4l+2}n(l+1)^{4l+3}n(l+2)$ configuration (Fig. 10.10).

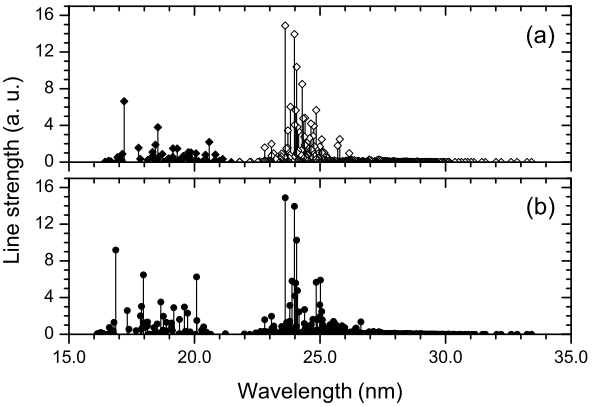

Fig. 10.10 Line strength distribution of transitions for Cd^{4+}: (**a**) $4p^5 4d^9$–$4p^6 4d^8$ (*solid diamonds*) and $4p^6 4d^7 4f$–$4p^6 4d^8$ (*open diamonds*); (**b**) $(4p^5 4d^9 + 4p^6 4d^7 4f)$–$4p^6 4d^8$. Calculations are made in the single-configuration and two-configuration HFR approximations

10.3.3 SEOS CI Influence on the Spectra, Corresponding to the Excitation from the Ground Level of Ion

The intensity of lines for the photoexcitation spectrum is proportional to the oscillator strength. The intensity of line for the emission spectrum is expressed [42]:

$$I\left(K\gamma - K_0\gamma'\right) = \frac{\sigma_{\mathrm{ex}}(K_0\gamma_0 - K\gamma)A(K\gamma - K_0\gamma')}{\sum_{\gamma''} A(K\gamma - K_0\gamma'')}, \tag{10.16}$$

where σ_{ex} is the photoexcitation cross section, A is the radiative transition probability, K_0 is the ground configuration, γ', γ'' are its levels and γ_0 is the lowest level, K means one of the two excited configurations in the single-configuration approximation or their superposition in the two-configuration approximation, γ is its level. The sum in the denominator corresponds to the total transition probability from γ level; for the considered cases only radiative transitions to the various levels of the ground configuration give contribution to this quantity.

In Fig. 10.11 such photoexcitation and emission spectra for the W^{q+} ions with a different number of electrons in the $4d^N$ shell are presented. Two features of them attract the attention: the similarity of both kinds of spectra and formation of NGIL only for some ions.

The similarity of the photoexcitation and emission spectra is not a self-explanatory result and means that the transitions from the excited configurations proceed mainly to the same ground level of the initial configuration. It is not typical of the spectra, calculated in the single-configuration approximation, thus, the transitions to the other levels are effectively suppressed by the two-configuration interaction.

The spectra of various W^{q+} ions demonstrate that CI SEOS does not always cause the narrowing of spectrum. This effect manifests itself very distinctly at large number of $4d$ electrons $N \geq 4$: the width of the group of intense lines does not exceed several percent of the whole energy interval of transition array (Table 10.2) and only very weak lines appear in the remaining part of spectrum. However, at

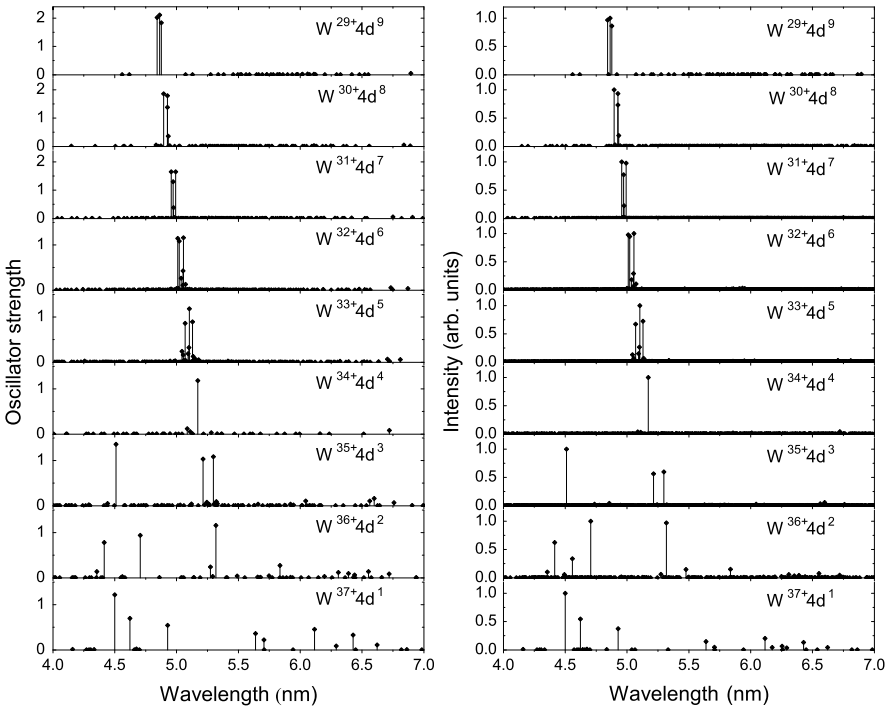

Fig. 10.11 Photoexcitation and emission spectra of W^{q+} ions, corresponding to $(4p^5 4d^{N+1} + 4p^6 4d^{N-1} 4f)$–$4p^6 4d^N$ transitions, after the photoexcitation from the ground level of the corresponding ion [43]. Calculations are made in the two-configuration HFR approximation

Table 10.2 Intervals of wavelengths of the whole emission spectrum, corresponding to transitions $(4p^5 4d^{N+1} + 4p^6 4d^{N-1} 4f)$–$4p^5 4d^N$, ($\Delta\lambda_s$) and those of the main group of lines which intensities exceed 5 % of the most intense line ($\Delta\lambda_{il}$) [43]

N	$\Delta\lambda_s$ (nm)	$\Delta\lambda_{il}$ (nm)	$\Delta\lambda_{il}/\Delta\lambda_s$ (%)
9	3.03	0.03	0.99
8	4.28	0.04	0.93
7	5.50	0.04	0.73
6	6.89	0.06	0.87
5	8.82	0.09	1.01
4	9.55	0.00	0
3	9.80	2.09	21.3
2	8.02	6.12	76.3
1	5.25	1.81	34.5

small number of electrons $N \leq 3$, the formation of NGIL does not take place at all—the intense lines remain distributed within a rather wide interval of wavelengths.

The reason of such a different influence of CI SEOS on the spectra of ions of the same element with the same open shell follows from the comparison of their

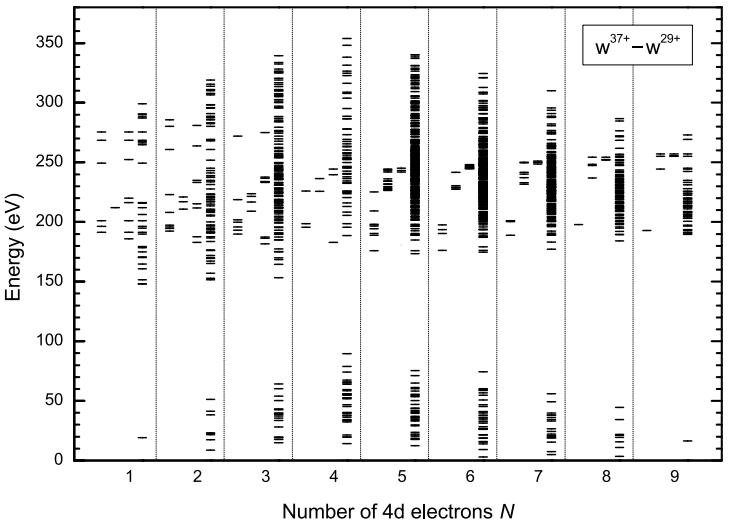

Fig. 10.12 Energy level diagram for W^{q+} ($q = 29$–37) ions [31]. The *columns of bars* at the *bottom part of diagram* represent all energy levels of the ground configuration $4p^6 4d^N$. At the *upper part of diagram*, the energy levels which can be excited from the lowest level of the ground configuration are plotted. For every ion, the *right column* represents all possible excited levels of $4p^5 4d^{N+1}$ and $4p^6 4d^{N-1} 4f$ configurations, the other columns represent only the energy levels with excitation cross sections exceeding 5 % of this value for the most excited level: the *first* (*second*) *column* gives such levels of $4p^5 4d^{N+1}$ ($4p^6 4d^{N-1} 4f$) configuration; the *third column* gives the most excited levels in the two-configuration approximation. Calculations are made in the HFR approximation

energy level spectra (Fig. 10.12). These results indicate that the formation of NGIL depends on the mutual positions of levels of the upper group, which are mainly populated by the excitation from the ground level. The necessary condition of this effect is that such levels of $4p^5 4d^{N+1}$ configuration should lie below such levels of $4p^6 4d^{N-1} 4f$ configuration. This condition is fulfilled at $N \geq 4$, when the $4d_{3/2}$ subshell is closed and the $4p_{1/2}$–$4d_{3/2}$ as well as $4p_{3/2}$–$4d_{3/2}$ transitions are forbidden. On decreasing a number of electrons N from 4 up to 3, such transitions become allowed, therefore the higher levels of $4p^5 4d^{N+1}$ configuration are populated and transitions to them are not canceled by CI SEOS.

This regularity is confirmed by calculations for the other elements and explains the variation of spectra in the isoelectronic sequences. Due to the similarity of the photoexcitation and emission spectra we will consider only one of them.

In the first ions, the $4f$ orbital is not yet essentially contracted and the excited levels of $4p^6 4d^{N-1} 4f$ configuration tend to lie below such levels of $4p^5 4d^{N+1}$ configuration, then the width of spectrum is rather large (Fig. 10.13). On increasing the ionization degree the levels of $4p^6 4d^{N-1} 4f$ configuration are shifted down and then spectra are dominated by NGIL. At large ionization degrees, three types of the variation of spectra can be distinguished. At $N \leq 3$, the emission spectrum tends to become wider with q (Fig. 10.13a). At $4 \leq N \leq 9$, the strong concentration of lines

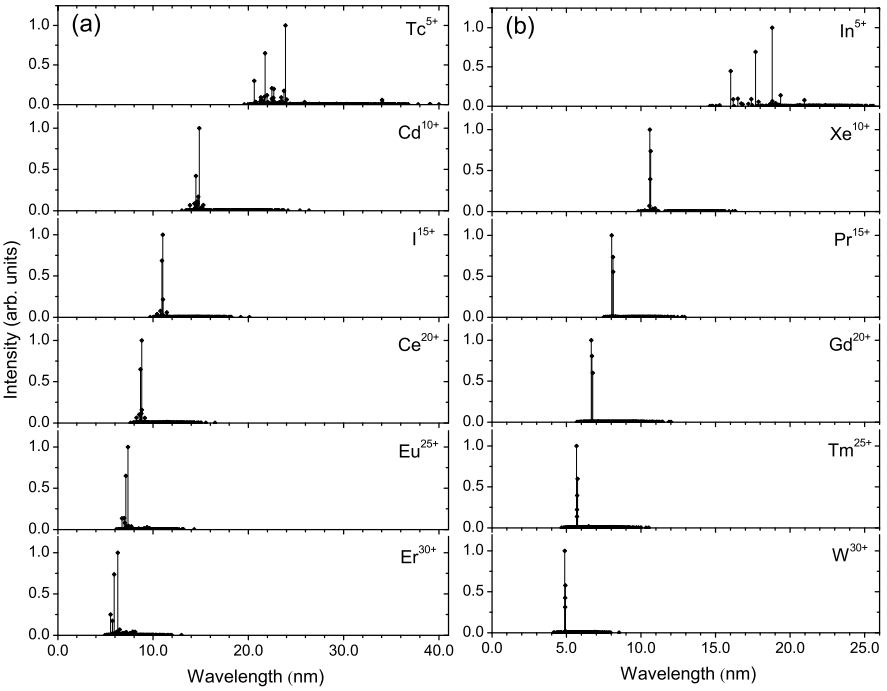

Fig. 10.13 Emission spectra, corresponding to $(4p^5 4d^3 + 4p^6 4d 4f)$–$4p^6 4d^2$ transitions, for the Sr isoelectronic sequence (**a**) and to $(4p^5 4d^9 + 4p^6 4d^7 4f)$–$4p^6 4d^8$ transitions for the Ru isoelectronic sequence (**b**) [31]. Spectra were photoexcited from the ground level. Results of calculation in the two-configuration HFR approximation

remains characteristic of highly charged ions due to the above indicated relativistic effect—the filling of the $4d_{3/2}$ subshell (Fig. 10.13b). The particularly narrow spectrum at various ionization degrees is obtained for $N = 5$ when the excitation takes place from the ground level with its total quantum number equal to zero (this essentially reduces a number of possible transitions).

These main regularities hold also for the spectra, corresponding to transitions (10.11). The necessary condition of the formation of NGIL is that all levels of $3s3p^{N+1}$ configuration, mainly excited from the ground level, must lie below the corresponding levels of $3s^2 3p^{N-1} 3d$ configuration. However, the open shells with a smaller orbital quantum number contain considerably smaller number of levels. Thus, some levels of $3s3p^{N+1}$ configuration at $N = 1$ and 2 are not related by the Coulomb interaction to the levels of $3s^2 3p^{N-1} 3d$ configuration; consequently, the corresponding lines are not canceled by CI (Fig. 10.14). The formation of NGIL is more expressed at a half-filled and an almost-filled $3p^N$ shell. In the isoelectronic sequences this effect begins at smaller ionization degrees than for transitions (10.12) and takes place up to about $q = 30$ (Fig. 10.15). Namely, in this interval of the isoelectronic sequence the intense lines of $3p$–$3d$ transitions are situated on the shorter wavelength side than the intense lines of $3s$–$3p$ transitions; at larger values of q,

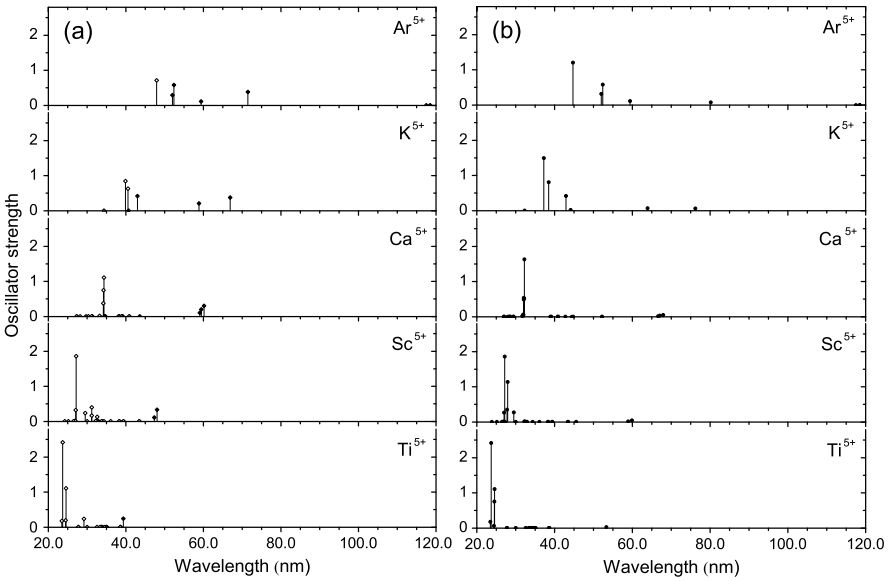

Fig. 10.14 Photoexcitation spectra corresponding to the transitions from the ground level of the $3s^2 3p^N$ configuration to the levels of the $3s3p^{N+1}$ and $3s^2 3p^{N-1}3d$ configurations at $N = 1$–5 and $q = 5$: (**a**) transitions to the levels of the $3s^2 3p^{N-1}3d$ (*open diamonds*) and of $3s3p^{N+1}$ (*solid diamonds*) configurations; (**b**) transitions to the same configurations in the two-configuration HFR approximation [32]

they begin to overlap and the spectrum becomes wider. The spectra of photoexcitation from the ground level and the inverse emission spectra are also rather similar due to the suppression by CI SEOS of transitions to the levels of upper terms of the ground configuration.

10.4 Conclusions

The formation of NGIL is typical of the electric dipole transitions between the configuration with a vacancy $nl^{4l+1}n(l+1)^{N+1}$ and the ground configuration $nl^{4l+2}n(l+1)^N$. Two different cases can be distinguished:

(i) The ground configuration has an open $3d^N$ or $4f^N$ shell. The strong Coulomb exchange interaction between the shells with the same principal quantum number separates the energy level spectrum of the excited configuration $nl^{4l+1}n(l+1)^{N+1}$ into two groups of levels with very different rates of transitions to/from $nl^{4l+2}n(l+1)^N$ configuration. This is the reason of the formation of NGIL on a short-wavelength side of the spectrum and manifests itself by giant resonances in the photoabsorption spectra of lanthanides and some iron group elements.

(ii) The ground configuration has an open $3p^N$ or $4d^N$ shell. Then also the configuration $nl^{4l+2}n(l+1)^{N-1}n(l+2)$ of the same complex exists and its strong

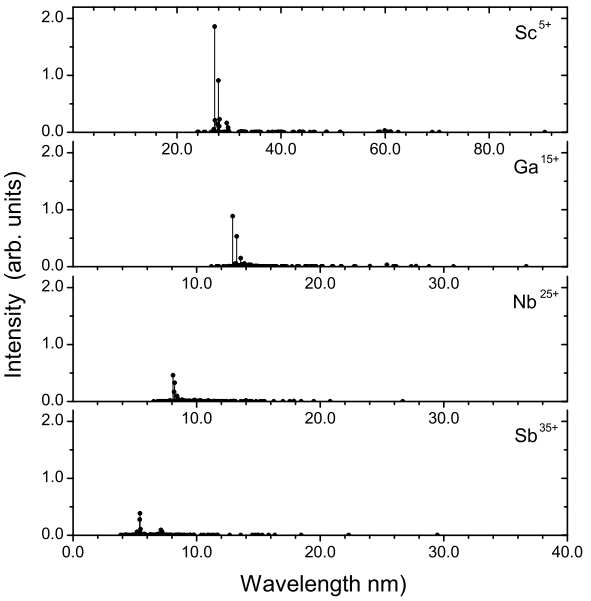

Fig. 10.15 Emission spectra of S-like ions at $q = 5$, 15, 25 and 35, corresponding to transitions $(3s3p^5 + 3s^2 3p^3 3d)$–$3s^2 3p^4$, after the photoexcitation from the ground level of $3s^2 3p^4$ configuration [32]. Calculations are made in the two-configuration HFR approximation

interaction with the $nl^{4l+1}n(l+1)^{N+1}$ configuration has an essential influence on both emission and photoexcitation spectra, corresponding to the transitions:

$$nl^{4l+2}n(l+1)^N - \left(nl^{4l+1}n(l+1)^{N+1} + nl^{4l+2}n(l+1)^{N-1}n(l+2)\right).$$

The main effect is also the formation of NGIL. When the whole array of transition probabilities is considered, CI SEOS enhances the shorter wavelength transitions from the higher configuration and quenches the longer wavelength transitions from the lower configuration. In the case of spectra, excited from the ground level of $nl^{4l+2}n(l+1)^N$ configuration, the necessary condition for the formation of NGIL is the following: all levels of $nl^{4l+1}n(l+1)^{N+1}$ configuration, mainly excited from the ground level, must lie below the corresponding levels of $nl^{4l+2}n(l+1)^{N-1}n(l+2)$ configuration. The exceptions are possible for simple configurations, which some terms are not related by the interconfiguration matrix elements.

There exists a similarity between the two mechanisms of the intensity concentration in the single-configuration and two-configuration approximations. In both cases the intensity is enhanced in the transitions involving the upper group of levels and is canceled in the transitions involving the lower group of levels. Both mechanisms are related to the specific structure of matrix elements of the Coulomb interaction operator: the possibility to express them in terms of transition amplitudes.

Cancellation of many lines means the existence of additional selection rule. For the single-configuration model such a rule for a number of vacancy-electron pairs was established using the hole-particle basis. The introduction of a new wavefunction basis and strict theoretical formulation of cancellation mechanism in the photoexcitation and emission spectra due to CI SEOS is an actual problem.

Acknowledgements This work was partially supported by the Research Council of Lithuania, contract No. MIP-61/2010 and by the European Communities under the contract of association between EURATOM and Lithuanian Energy Institute.

References

1. D.R. Beck, C.A. Nicolaides, Phys. Rev. A **26**, 857 (1982)
2. T.M. Zimkina, V.A. Fomichev, S.A. Gribovskii, I.I. Zhukova, Sov. Phys., Solid State **9**, 1128 (1967)
3. J. Sugar, Phys. Rev. B **5**, 1785 (1972)
4. I. Glembockis et al., Litov. Fiz. Sb. **12**, 35 (1972) (in Russian)
5. J.P. Connerade, J.M. Esteva, R.C. Karnatak (eds.), *Giant Resonances in Atoms, Molecules and Solids* (Plenum Press, New York, 1986)
6. M. Richter et al., Phys. Rev. A **40**, 7007 (1989)
7. J.P. Connerade, Contemp. Phys. **19**, 415 (1978)
8. S. Kučas, R. Karazija, Phys. Scr. **58**, 220 (1998)
9. S. Kučas, R. Karazija, J. Phys. B **24**, 2925 (1991)
10. A. Bernotas, R. Karazija, J. Phys. B **34**, L741 (2001)
11. M. Meyer et al., Z. Phys. D **2**, 347 (1986)
12. M. Martins, K. Godehusen, T. Richter, Ph. Wernet, P. Zimmermann, J. Phys. B **39**, R79 (2006)
13. C. Froese Fischer, J. Quant. Spectrosc. Radiat. Transf. **8**, 755 (1968)
14. R.D. Cowan, J. Phys. (Paris) **31**, C4–191 (1970)
15. M. Aymar, Nucl. Instrum. Methods **110**, 211 (1973)
16. G. O'Sullivan, P.K. Carroll, J. Opt. Soc. Am. **71**, 227 (1981)
17. P.K. Carroll, G. O'Sullivan, Phys. Rev. A **25**, 275 (1982)
18. J. Bauche, C. Bauche-Arnoult, M. Klapisch, P. Mandelbaum, J.L. Schwob, J. Phys. B **20**, 1443 (1987)
19. J. Bauche et al., Phys. Rev. A **28**, 829 (1983)
20. G. O'Sullivan et al., in *EUV Sources for Lithography*, ed. by V. Bakshi (SPIE, Bellingham, 2006)
21. S.S. Churilov, R.R. Kildyarova, A.N. Ryabtsev, S.V. Sadovsky, Phys. Scr. **80**, 045303 (2009)
22. J. White et al., J. Appl. Phys. **98**, 113301 (2005)
23. S.S. Churilov, A.N. Ryabtsev, Phys. Scr. **73**, 614 (2006)
24. R. Karazija, S. Kučas, A. Momkauskaitė, J. Phys. D **39**, 2973 (2006)
25. R. D'Arcy et al., Phys. Rev. A **79**, 042509 (2009)
26. D. Kilbane, G. O'Sullivan, J. Appl. Phys. **108**, 104905 (2010)
27. 2011 International Workshop on EUV Lithography, Maui, 2011. www.euvlitho.com
28. R. Radtke et al., Phys. Rev. A **64**, 012720 (2001)
29. C. Biedermann, R. Radtke, R. Seidel, T. Pütterich, Phys. Scr. T **134**, 014026 (2009)
30. T. Pütterich et al., Plasma Phys. Control. Fusion **50**, 085016 (2008)
31. S. Kučas, R. Karazija, V. Jonauskas, A. Momkauskaitė, J. Phys. B **42**, 205001 (2009)
32. R. Karazija, A. Momkauskaitė, L. Remeikaitė-Bakšienė, J. Phys. B **44**, 035002 (2011)
33. R.D. Cowan, *The Theory of Atomic Structure and Spectra* (University of California Press, Berkeley, 1981)
34. M.F. Gu, Can. J. Phys. **86**, 675 (2008)
35. I.P. Grant, B.J. McKenzie, P.H. Norrington, D.F. Mayers, N.C. Pyper, Comput. Phys. Commun. **21**, 207 (1980)
36. A. Bernotas, Doctoral Thesis, Vilnius, 1990
37. S. Kučas, V. Jonauskas, R. Karazija, Phys. Scr. **51**, 566 (1995)
38. S.S. Churilov, A.N. Ryabtsev, Opt. Spectrosc. **101**, 169 (2006)
39. S. Kučas, V. Jonauskas, R. Karazija, A. Momkauskaitė, Lith. J. Phys. **47**, 249 (2007)

40. R. Radtke, C. Biedermann, J.L. Schwob, P. Mandelbaum, R. Doron, Phys. Rev. A **64**, 012720 (2001)
41. D. Kilbane, G. O'Sullivan, Phys. Rev. A **82**, 062504 (2010)
42. R. Karazija, *Introduction to the Theory of X-Ray and Electronic Spectra* (Plenum Press, New York, 1996)
43. V. Jonauskas, S. Kučas, R. Karazija, J. Phys. B **40**, 2179 (2007)